

Solitons in a Channel Emerging from a Three-Dimensional Initial Wave.

S. PIERINI (*)

Department of Engineering Sciences, University of Florida - Gainesville, FL

(ricevuto il 16 Luglio 1986)

Summary. — An implicit, three-time level, finite-difference scheme is presented which solves the initial-boundary-value problem for a regularized Kadomtsev-Petviashvili equation, modelling the evolution of a variety of wave systems for which weak dispersive, nonlinear and three-dimensional effects are taken into account. Linear and nonlinear tests are performed to test the scheme and the numerical results are found to compare accurately with known theoretical solutions. The evolution of a localized weakly three-dimensional initial condition in a channel is then studied. In all cases the numerical experiments show that the wave tends to a two-dimensional state: for initial waves with positive net volume two-dimensional solitons rapidly emerge. This behaviour agrees with laboratory experiments performed by different authors. Moreover, the radiation yields three-dimensional patterns similar to Genus 2, solutions of the KP equation.

PACS. 92.10. — Physics of the ocean.

1. — Introduction.

Much effort has been devoted in recent years to the study of the Kadomtsev-Petviashvili (KP ⁽¹⁾) equation

$$(1) \quad (\eta_t + c\eta_x + \alpha\eta_{xxx} + \beta\eta\eta_x)_x + \frac{c}{2}\eta_{yy} = 0,$$

(*) Permanent and present address: Istituto di Oceanologia, Istituto Universitario Navale, Via Acton 38, 80133 Napoli (Italy).

(1) B. B. KADOMTSEV and V. I. PETVIASHVILI: *Sov. Phys. Dokl.*, **15**, 539 (1970).

which represents the natural generalization of the Korteweg-de Vries (KdV) equation

$$\eta_t + c\eta_x + \alpha\eta_{xxx} + \beta\eta\eta_x = 0$$

to the case of weakly nonlinear and weakly dispersive wave systems for which weak three-dimensionality is allowed (the constants c , α and β depend on the physical problem in question). The KP equation was first proposed in (1) to study the stability of KdV solitons with respect to transverse perturbations. A detailed derivation of (1) for gravity and capillary-gravity waves is given in ABLOWITZ and SEGUR (2). KRICHEVER (3) first noticed that the KP equation has exact, periodic solutions given by

$$(2) \quad \eta(x, y, t) = 2 \frac{\partial^2}{\partial x^2} \ln \Phi_N,$$

where Φ_N is the Riemann theta function of Genus N . These solutions have been discussed in detail by DUBROVIN (4) and SEGUR and FINKEL (5). The solution for $N = 1$ corresponds to a cnoidal wave travelling in a direction slightly tilted with respect to the x -axis. For $N = 2$, (2) gives a class of biperiodic (two real periods) waves of permanent, hexagonlike form. These waves have been very clearly reproduced in laboratory experiments (J. L. HAMMACK, private communication). For $N > 2$ the form of the wave is time-dependent.

However, from a physical viewpoint it is also of great relevance to investigate the basic features of the evolution of a localized initial condition. The KP equation is of the IST (inverse scattering transform, see (6) for the KdV equation) type and indeed a generalized version of the IST applicable to (1) has been developed both for capillary-gravity and gravity waves (7,8). However solutions of (1) in physically interesting cases are not yet available, so at this stage numerical computations appear to be the only means to get some insight into the 3D features of the wave evolution.

A numerical scheme for a generalized KP equation was proposed by LIU *et al.* (9). It is based on a spectral representation of the field and is very accurate in modelling the scattering of energy into the higher harmonics of a

(2) M. J. ABLOWITZ and H. SEGUR: *J. Fluid Mech.*, **92**, 691 (1979).

(3) I. M. KRICHEVER: *Funct. Anal. Appl.*, **10**, 144 (1976).

(4) B. A. DUBROVIN: *Russ. Math. Surveys*, **36**, 11 (1981).

(5) H. SEGUR and A. FINKEL: *Stud. Appl. Math.*, **73**, 183 (1985).

(6) C. S. GARDNER, J. M. GREENE, M. D. KRUSKAL and R. M. MIURA: *Commun. Pure Appl. Math.*, **27**, 97 (1974).

(7) V. E. ZACHAROV and S. V. MANAKOV: *Phys. Rev. (Sov. Scient. Rev.)*, **1**, 133 (1979).

(8) M. J. ABLOWITZ, D. BAR YAACOV and A. S. FOKAS: *Stud. Appl. Math.*, **69**, 135 (1983).

(9) P. L. F. LIU, S. B. YOON and J. T. KIRBY: *J. Fluid Mech.*, **153**, 185 (1985).

monochromatic wave travelling over a 3D topography. A different approach is represented by a difference scheme solving the initial-boundary-value problem for $\eta(x, y, t)$ without resorting to a spectral decomposition of the field. Such a method would be particularly suitable for modelling the evolution of an initial condition with a broad Fourier spectrum. In this respect very recently KATSIS and AKYLAS⁽¹⁰⁾ have proposed an explicit, two-time level finite-difference scheme for a forced KP equation.

In this paper we present an implicit, three-time level finite-difference scheme solving a model equation that is basically equivalent to the KP equation but that, presumably, has better properties in numerical computations. This equation will be discussed in sect. 2 and the corresponding numerical scheme will be presented in sect. 3. In sect. 4 a series of linear and nonlinear tests is presented where some theoretical solutions are found to correspond with the numerical ones.

In sect. 5, 6 we study wave evolution in a rectangular channel for weakly three-dimensional initial conditions of Gaussian form in both the x and y directions. The results show very clearly that for a sufficiently energetic wave packet, 2D KdV solitons rapidly emerge and that the three-dimensionality of the initial wave is left in the radiation field. This evolution behaviour is not surprising having in mind what RUSSELL⁽¹¹⁾ tells on his famous first encounter with the KdV soliton:

« ..., when the boat suddenly stopped—not so the mass of water in the channel, which it had put in motion; it accumulated round the prow of the vessel in a state of violet agitation, then suddenly leaving it behind, rolled forward with great velocity, assuming the form of a large solitary elevation, ... »

The initial « mass of water » observed by RUSSELL was very likely three-dimensional and still evolved a wave that was essentially two-dimensional.

Finally in sect. 7 a comparison of the present numerical results with experiments performed by different authors and with other numerical studies will be discussed.

2. – The KP equation and an alternative model equation.

A linear, nondispersive wave travelling in the positive x -direction,

$$(3) \quad \eta = A \exp [i(kx - \omega t)]$$

⁽¹⁰⁾ C. KATSIS and T. R. AKYLAS: submitted to *J. Fluid Mech.* (1986).

⁽¹¹⁾ J. S. RUSSELL: Report Meeting British Association Advancement of Science 14th, York, p. 311 (1845).

is solution of the equation

$$(4) \quad \eta_t + c\eta_x = 0,$$

where $c = \omega/k = \text{const}$ is the nondispersive phase speed. If the direction of propagation of the wave forms a small angle with the x -axis, namely if

$$(5) \quad (k_y/k_x)^2 \ll 1,$$

one has

$$\omega = ck \simeq c \left(k_x + \frac{k_y^2}{2k_x} \right).$$

Taking this expression into account, from (3) one can derive

$$(6) \quad \eta_t = -c\eta_x - i c \eta_{yy} / (2k_x).$$

Differentiating (6) with respect to x one gets

$$(7) \quad (\eta_t + c\eta_x)_x + \frac{c}{2} \eta_{yy} = 0.$$

This is basically Kadomtsev-Petviashvili's derivation of (7). Assuming that the dispersive and nonlinear terms add to the linear advective term $c\eta_x$, one recovers the KP equation (1), which can however be derived rigorously⁽²⁾.

Returning to the 2D case, BENJAMIN *et al.* (12) proposed a model equation, first used by PEREGRINE (13). It can be obtained from the KdV equation by substituting one x -derivative with one time derivative in the dispersive term according to (4) (note that (4) gives the leading-order effects in the KdV equation):

$$(8) \quad \eta_t + c\eta_x - \frac{\alpha}{c} \eta_{xxt} + \beta \eta \eta_x = 0.$$

Equation (8) is known as the PBBM (from (12,13)) or RLW (regularized long wave) equation. In (12) it is stressed that (8) has the same formal justification as KdV and has a dispersion relation which unlike that of KdV does not allow spurious short waves to propagate rapidly along the negative x -direction (this is a particularly useful property in numerics where one has to impose some boundary condition at the left x -boundary). It was therefore suggested that (8)

(12) T. B. BENJAMIN, J. L. BONA and J. J. MAHONY: *Philos. Trans. R. Soc. London, Ser. A*, **272**, 47 (1972).

(13) D. H. PEREGRINE: *J. Fluid Mech.*, **25**, 321 (1966).

could be a better model equation for numerical applications. Moreover BONA and SMITH⁽¹⁴⁾ later proved that, under assumptions that are also required for the derivation of both equations, the solutions of the KdV and PBBM initial-value problems are pointwise close to each other. Note however that (8) is not solvable by IST (OLVER⁽¹⁵⁾ has proved that it admits only three conservation laws).

Here we propose the evolution equation that can be obtained from the KP equation by introducing the same substitution that links the PBBM to the KDV equation, *i.e.*

$$(9) \quad \left(\eta_t + c\eta_x - \frac{\alpha}{c}\eta_{xxt} + \beta\eta\eta_x \right)_x + \frac{c}{2}\eta_{yy} = 0,$$

which might be termed the regularized KP equation. We conjecture that the solutions of (1) and (9) for the same initial and boundary conditions should lie close to each other and that, presumably, (9) has better properties than (1) as far as its numerical resolution is concerned, just like the PBBM equation has some advantage with respect to the KdV equation in numerical applications. However, eq. (9) will not be solvable by IST.

In the remainder of the paper we present a finite-difference scheme for eq. (9): it will be tested and then applied to the study of the evolution in a channel of a localized hump of water.

3. - The numerical scheme.

In a paper on the development of undular bores, PEREGRINE⁽¹³⁾ presented a two-time level, implicit finite-difference scheme for eq. (8). More recently EILBECK and Mc GUIRE⁽¹⁶⁾ developed a series of first and second-order, two- and three-level schemes for the same equation. Their second-order, three-level scheme (which we shall heretofore call EMG) is the most sophisticated and constitutes a substantial improvement over that of⁽¹³⁾. They also derived a condition for stability and found their scheme to always be unconditionally stable for any problem of practical significance. In the following we shall present a three-dimensional generalization of the EMG scheme for eq. (9).

Under the assumption

$$(10) \quad \lim_{x \rightarrow \infty} \eta = 0,$$

⁽¹⁴⁾ J. L. BONA and R. SMITH: *Philos. Trans. R. Soc. London, Ser. A*, **278**, 555 (1975).

⁽¹⁵⁾ P. J. OLVER: *Math. Proc. Cambridge Philos. Soc.*, **85**, 143 (1979).

⁽¹⁶⁾ J. C. EILBECK and G. R. McGUIRE: *J. Comput. Phys.*, **19**, 43 (1975).

(9) can be integrated to give

$$(11) \quad \eta_t + c\eta_x - \frac{\alpha}{c}\eta_{xxt} + \beta\eta\eta_x - \frac{c}{2} \int_x^\infty \eta_{yy} dx' = 0.$$

For gravity waves

$$c = (gH)^{\frac{1}{2}}, \quad \alpha = H^2 c/6, \quad \beta = \frac{3}{2} \left(\frac{g}{H}\right)^{\frac{1}{2}},$$

where H is the water depth and g the acceleration of gravity. So, through the scaling

$$\eta = HE, \quad x = HX, \quad y = HY, \quad t = \left(\frac{H}{g}\right)^{\frac{1}{2}} T,$$

we get a nondimensional version of (11):

$$(12) \quad E_T + E_X - \frac{1}{6} E_{xxt} + \frac{3}{2} EE_X - \frac{1}{2} \int_x^\infty E_{YY} dX' = 0.$$

Let us define

$$E_{i,j}^s = E(iDX, jDY, sDT).$$

In the scheme below we have exploited the weakness of the three-dimensionality of the physical problem. In fact we have solved (12) in a rectangular domain by applying the EMG scheme at a given time in every line $j = \text{const}$ for the PBBM equation modified by the presence of the additional term $-\frac{1}{2} \int_x^\infty E_{YY} dX'$ modelling the 3D effects.

Starting from $\{E_{i,j}^{s-1}\}$ and $\{E_{i,j}^s\}$ we evaluate $\{E_{i,j}^{s+1}\}$ by solving the M linear systems

$$(13) \quad \begin{cases} (E_{i,j}^{s+1} - E_{i,j}^{s-1})/(2DT) + (1 + \frac{3}{2} E_{i,j}^s)(E_{i+1,j}^s - E_{i-1,j}^s)/(2DX) - \\ \quad - (E_{i+1,j}^{s+1} - 2E_{i,j}^{s+1} + E_{i-1,j}^{s+1} - E_{i+1,j}^{s-1} + 2E_{i,j}^{s-1} - E_{i-1,j}^{s-1})/(12DTDX^2) - \\ \quad - \frac{1}{2} \text{INT}_i[(E_{m,j+1}^s - 2E_{m,j}^s + E_{m,j-1}^s)/DY^2] = 0, \quad i = 2, \dots, N-1, \\ E_{1,j}^{s+1} = a, \\ E_{N,j}^{s+1} = 0, \end{cases}$$

for $j = 1, \dots, M$; as for the x -boundary conditions, a will be specified later, while condition $E_{N,j}^{s+1} = 0$ is essential because of (10), and during the evolution the leading edge of the wave has always been well behind the right x -boundary.

The operator INT is defined as

$$\text{INT}_i[A_m] = \int_{iDX}^{NDX} A(X') dX', \quad X' = mDX,$$

where m is a dummy subscript (we have used a trapezoidal integration).

The scheme (13) needs two initial levels of starting values, $\{E_{i,j}^0\}$ and $\{E_{i,j}^1\}$. The first is provided by the initial condition

$$(14) \quad E_{i,j}^0 = \mathcal{E}_{i,j}$$

and the second can be obtained from (14) by making use of the two-level « modified Peregrine scheme » described in ⁽¹⁶⁾, modified by the integral term—as in (13)—containing the field $\{E_{i,j}^0\}$.

The system (13) is tridiagonal, so it can be quickly solved by means of a standard iterative procedure. Moreover, the disadvantage of the implicitness of the scheme (which is intrinsic for the PBBM or (9) equation because of the presence of a time derivative in the dispersive term) is compensated by the better stability properties common to any implicit scheme.

4. — Numerical tests.

Some exact periodic solutions of (12) are known ⁽⁵⁾, but it is difficult to reproduce them because of the high complexity in computing their analytical form. Instead we have performed tests by using solutions of the KdV equation travelling along a direction forming a small angle with x , namely obliquely propagating plane waves and solitons. Although physically trivial (they are 2D solutions in an appropriate co-ordinate system), such waves are not trivial from a mathematical point of view. First the results of linear tests on plane waves will be presented. We shall then discuss nonlinear tests on oblique solitons.

Linear sinusoidal waves have been generated along the left x -boundary $i = 1$ by defining the fields $E_{1,j}^s$ in (13) as follows:

$$(15) \quad \begin{cases} E_{1,j}^s = A \cos\left(\frac{\pi j}{M} - \omega sDT\right) f(T), \\ f(T) = \{\sin(\pi T/2T_0), T < T_0; \quad 1, T > T_0\}. \end{cases}$$

This is a sinusoidal wave travelling along the line $i = 1$, with a wave-length λ_y equal to the width of the channel $L_y = MDY$. It has been smoothed during the initial time $T_0 = 2$ by the function $f(T)$. We have imposed y -periodic

boundary conditions, this being possible thanks to the condition $\lambda_y = L_y$. Moreover a very small amplitude, $A = 0.0001$, was chosen in order to be in the linear regime. The outgoing wave has to travel obliquely in order to match the field at $x = 0$. The theoretical angle φ_t that the wave crests should form with the y -axis depends on ω through the formula

$$(16) \quad \varphi_t = \arcsin(2\pi/kL_y),$$

where the wave number k is the first positive root of the dispersion relation

$$\omega = k - k^3/6.$$

We have performed a series of 6 tests using the frequencies $\omega = 0.3, 0.4, 0.5$ and choosing DY (and so L_y) in such a way that the theoretical angle given by (16) had the value $\varphi_t = 10^\circ, 20^\circ$ for each frequency. We have used the values $DX = DT = 0.25$, $M = 17$, N was continuously updated in order to satisfy condition (10) and the runs were carried out up to $T = 75$. In all cases an accurate agreement between φ_t and the observed angles φ_o was found. In fig. 1a), b) the lines of constant elevation for $\omega = 0.4$, $\varphi = 10^\circ, 20^\circ$ are given at $T = 75$.

Nonlinear tests have been performed by following the evolution of the initial condition

$$(17) \quad \mathcal{E}(X, Y) = A \operatorname{sech}^2 \left[p(A) \frac{(3A)^{\frac{1}{2}}}{2} \mathbf{KX} \right],$$

where \mathbf{K} is a unit vector that forms an angle φ with the x -axis. The function $p(A)$ would be 1 for (1), but as we have solved eq. (9) we have chosen the solitary wave solution of the PBBM equation for which $p(A) = (1 + A/2)^{-\frac{1}{2}}$. However, the difference between the two cases is virtually negligible. If the evolution of (17) were correct the lines $E = \text{const}$ should travel with the theoretical speed

$$c_t = 1 + A/2$$

along the direction given by \mathbf{K} . As for the y -boundary conditions, they cannot be periodic in this case, and a natural choice would be the free-slip condition along $y = 0, L_y$, that would model the propagation of the wave along a real, rectangular channel. With this choice, however, we have observed the gradual growth of stems in the vicinity of the lateral walls, this being physically correct because of the oblique propagation. However, as we were only interested in the propagation far from the boundaries, artificial boundary conditions have been imposed so that the deformation of the soliton away from the walls was

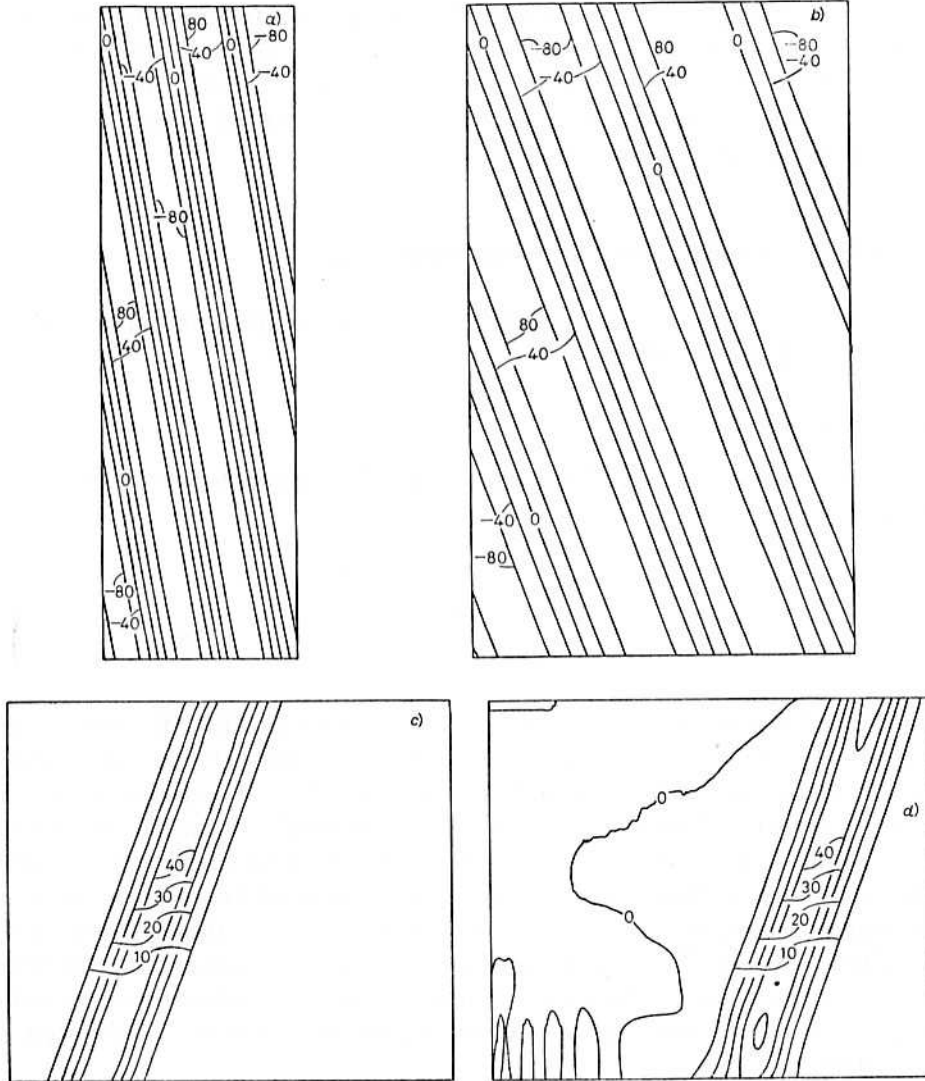


Fig. 1. - a), b) Lines of constant elevation ($\bar{E} = 1000 \cdot E$) for the linear sinusoidal waves generated at $x = 0$ in the tests with $\omega = 0.4$, $\varphi = 10^\circ$ and $\varphi = 20^\circ$ at $T = 75$. The number of grid points along x in the figure (n_{gr}) is 100. c), d) Lines of constant elevation for the oblique soliton in the test with $A = 0.05$ and $\varphi = 20^\circ$ at $T = 0$ and at $T = 25$, with special boundary conditions ($n_{\text{gr}} = 300$).

minimized. We have chosen to approximate $E_{YY}|_{j=1}$ with $E_{YY}|_{j=2}$ and $E_{YY}|_{j=M}$ with $E_{YY}|_{j=M-1}$.

We have performed a series of 6 tests using the amplitudes $A = 0.05, 0.2$ and the angles $\varphi = 10^\circ, 20^\circ, 30^\circ$. We have used the values $DX = DT = 0.25$, $M = 17$, $N = 350$, $a = 0$ in (13) and the runs were carried out up to $T = 25$.

Also for these nonlinear tests we have found an accurate agreement between theoretical and observed values e_i and e_0 . In fig. 1*c*), *d*) the contour lines for the case $A = 0.05$, $\varphi = 20^\circ$ are given at $T = 0$ and $T = 25$. In fig. 1*d*) we can notice some radiation from the walls. In the central region, however, the form of the soliton is virtually unchanged.

5. - Solitons emerging from 3D initial conditions.

In this section we will discuss the evolution of localized initial conditions in a rectangular channel.

Initial conditions.

We have chosen to model the initial conditions through the 3D Gaussian function

$$(18) \quad \mathcal{E}(X_1, X_2) = A \exp \left[- \sum_{i,j=1}^2 \delta_{ij} (X_i - \bar{X}_i)(X_j - \bar{X}_j) / (2S_i S_j) \right],$$

$$(\delta)_{i,j} = \begin{pmatrix} 1 & \delta \\ \delta & 1 \end{pmatrix}.$$

We emphasize that, since the KP equation—like KdV or PBBM—models the unidirectional (or « quasi-unidirectional » because of the 3D dynamics) propagation of long waves, (18) represents a wave that at $T = 0$ is already travelling along the positive x -direction with the long wave speed. It can be seen either as the result of the evolution of an initially steady wave packet (that would also give rise to another wave travelling along the opposite direction) or as a disturbance generated by a moving solid boundary, *e.g.* a ship moving down a channel (see sect. 7). Thanks to the unidirectional propagation, we have « followed » the wave by choosing a Galilean frame of reference moving with speed $c = 1$ (this implies a shift of one x -grid point for each time step if $DX = DT$).

Boundary conditions.

At the lateral boundaries the free-slip conditions

$$\left. \frac{\partial E}{\partial Y} \right|_{j=1, M} = 0$$

have been applied. At $X' = NDX$ ($X' = X - T$) we have imposed $E = 0$ (see (13)) and have chosen $N = 350$ —although the wave front never reached $X' = 300DX$ —in order to satisfy (10) rigorously. The boundary condition at $X' = 0$ is more critical. With $a = 0$ in (13) we have observed that as soon as the ra-

diation of (18) approaches $X'=0$ instabilities develop close to the lateral walls and remain confined within a narrow strip, say $0 < X' < 10$ (however their presence does not affect the evolution of the wave front even at very large times). We have, therefore, got rid of them by performing a shift of $n = 15/DX$ grid points at $T = 5$, by which time the instabilities were fully developed.

After this cut-off, $a = 0$ behaves as a very good radiation condition. In order to check this we have performed runs that differed only in the position of the centre of (18), \bar{X} . The difference between the values of E at a given point $(\bar{X}' - \Delta X', Y)$ was virtually negligible despite the fact that the distance of this point from the left x -boundary were different in the various cases (only at $i = 1, \dots, 5$ the values of E differed because E must vanish at $i = 1$). If the field «felt» the boundary, these values of E should differ from case to case.

Case A). We have chosen the following values: $DX = DT = 0.25$, $M = 17$, $N = 350$, $\bar{X} = 25$, $T_{\max} = 300$ (common to all the experiments) and $L_v = 50$, $\delta = 0$, $A = 0.2$, $S_1 = 3.75$, $S_2 = 12$. The characteristic length scales of the initial wave satisfy condition (5) (weak three-dimensionality), where for (18)

$$k_i \approx S_i^{-1}, \quad i = 1, 2.$$

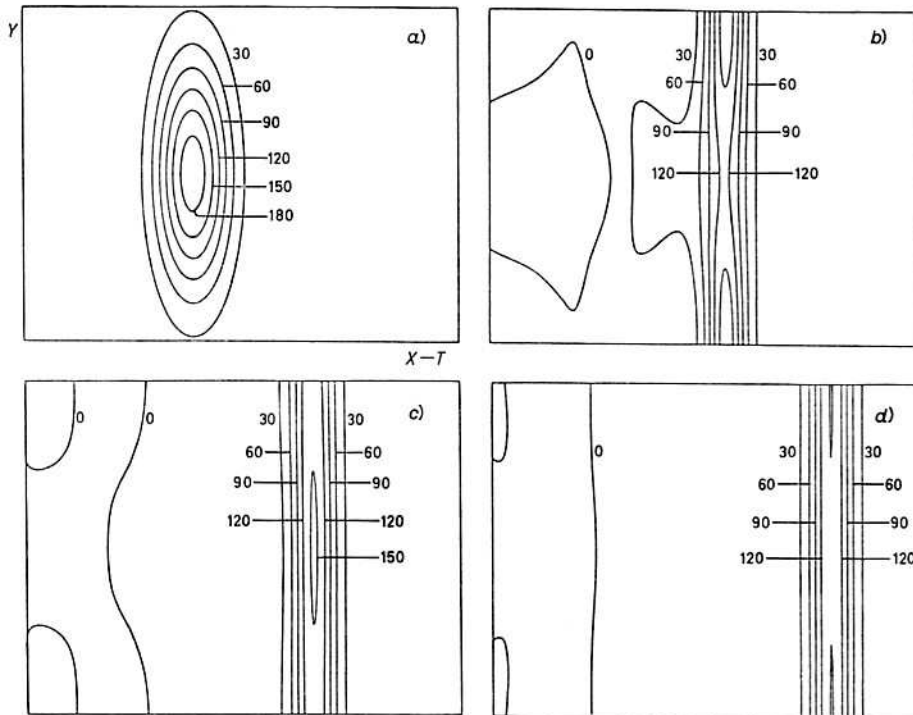


Fig. 2. - Contour lines of $\bar{E} = 1000 \cdot E$ in case A) (see text) at $T = 0$ (a), $T = 100$ (b), $T = 200$ (c) and $T = 300$ (d) ($n_{\text{tr}} = 250$).

Figure 2 shows that the initial 3D wave gives rise to a 2D soliton as a result of a 2D adjustment process. Condition (19) prescribing no flux through the lateral boundaries implies that the lines of constant elevation be perpendicular to the walls, and this in turn leads such lines to become straight in a rectangular channel (see also case *B*) for the role played by nonlinearities in this process). A small part of the energy goes into a 3D radiation field formed by the reflection of oblique Fourier components of the initial wave at the lateral boundaries. These 3D patterns yield some similarity with the Genus 2 solutions of (12) (*). It appears natural to regard this radiation field as the 3D counterpart of the linear dispersive tail typical of the 2D KdV evolution.

In the next four cases we will modify some parameters in order to analyse their effect on the global evolution. In particular, in cases *B*), *C*) the role of the walls in the development of the 2D KdV wave will be considered.

Case B). In this experiment the main axis of the double Gaussian forms a small angle with the lines $X = \text{const}$ ($\delta = 0.62$). The final state still contains a 2D soliton, however at the intermediate times one can see that the inclination of the wave first leads to the formation of a Mach stem near the left-hand wall with a corresponding accumulation of energy (fig. 3*b*). The speed of this region of the wave increases as a result of nonlinear effects, thus surpassing

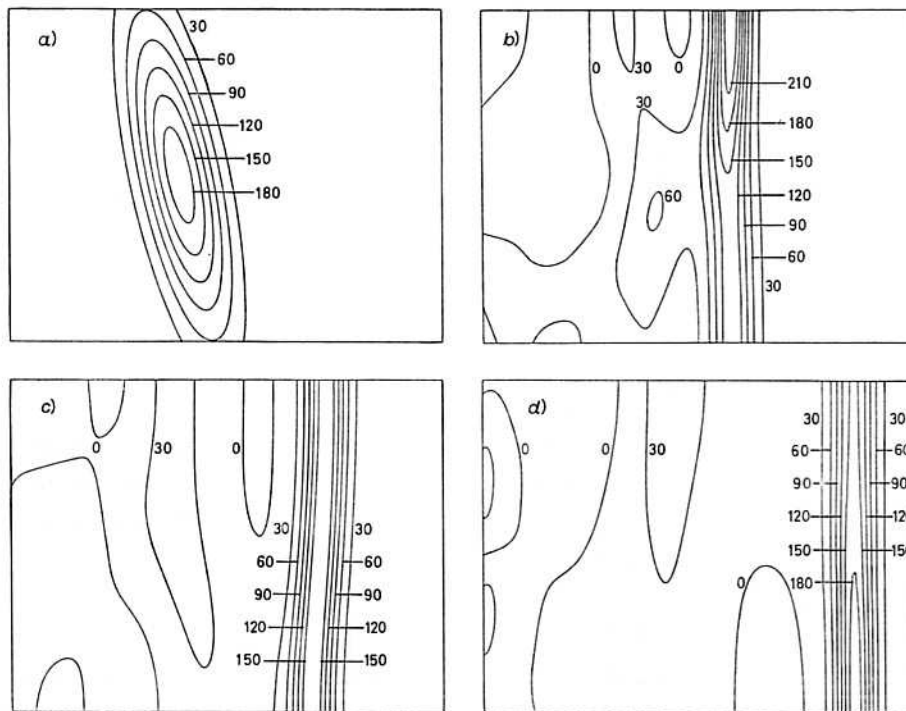


Fig. 3. - Contour lines of \tilde{E} in case *B*) (see text; $n_{\text{fig}} = 250$).

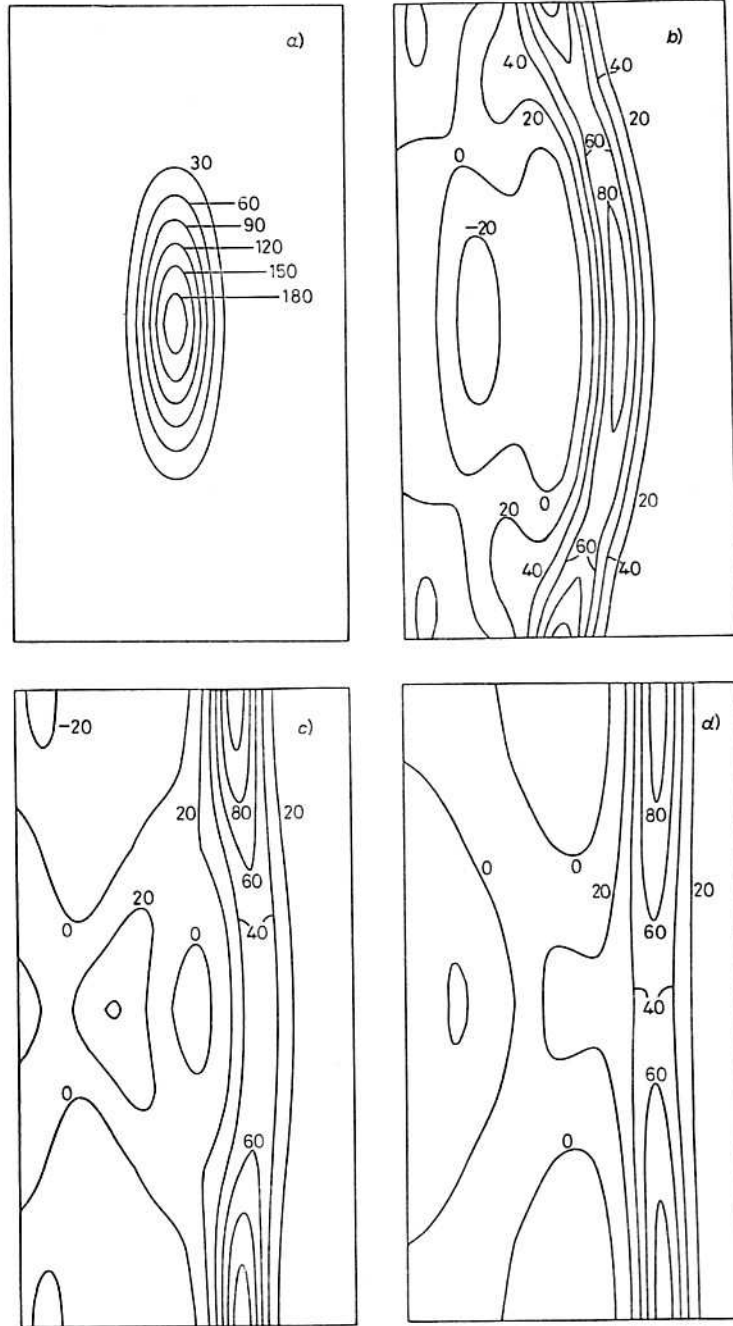


Fig. 4. - Contour lines of \tilde{E} in case C) (see text; $n_{11z} = 200$).

the right side of the wave and leading to an opposite but smaller inclination (fig. 3e)). This mechanism is repeated until the contours are exactly normal to the walls.

Case C). This case differs from case A) in that here the width of the channel is doubled ($L_y = 100$). Also in this case (fig. 4) the final state is 2D but the time necessary for attaining this asymptotic state is greater. This is because it takes longer for the wave to reach the boundaries.

6. - 2D waves emerging from 3D positive linear and negative initial conditions.

In this section we will consider the propagation of 3D positive linear and negative initial conditions.

Case D). It is well known that if the Ursell number of a positive 2D initial condition is much less than unity, the evolved wave will take the form of the

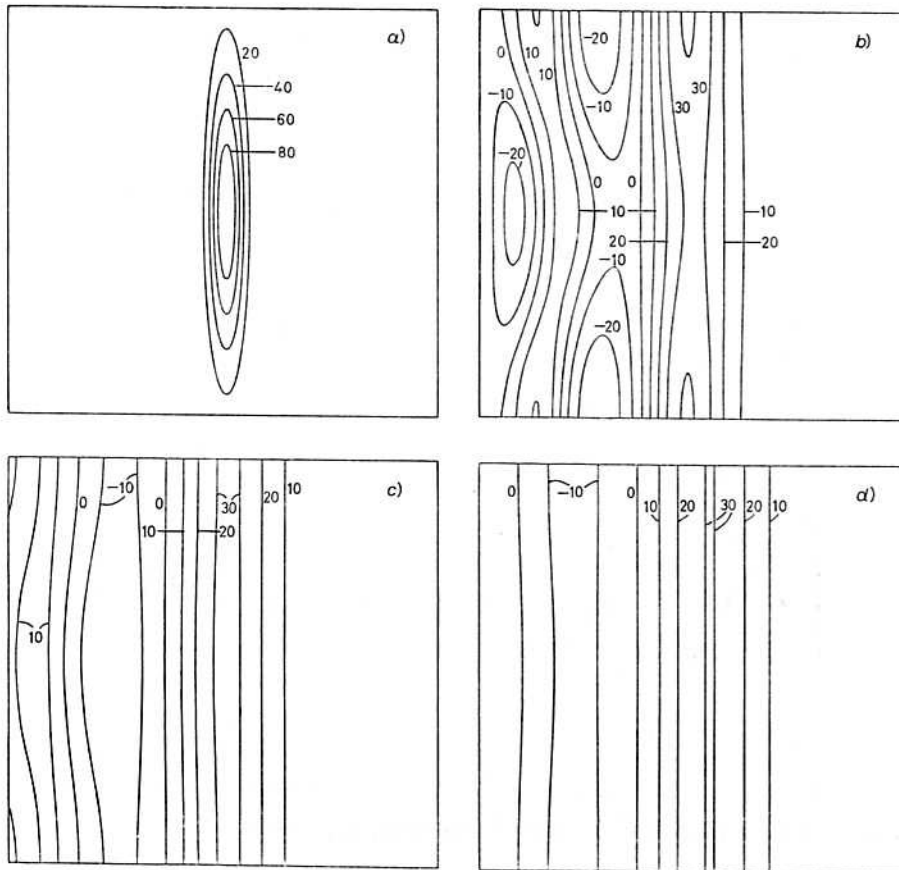


Fig. 5. - Contour lines of \tilde{E} in case D) (see text; $n_{11g} = 200$).

Airy function. This will still evolve into a single soliton but after a time scale that is much larger than that required in cases in which $U_0 > 1$ ⁽¹⁷⁾. In fig. 5 the weakly 3D generalization of this case is considered. The parameters are the same as in case A) except for $A = 0.1$ and $S_1 = 1.5$. The wave loses its 3D structure and yields very soon the Airy wave front.

Case E). If the initial condition is negative the evolution will not lead to solitons but to an oscillatory wave ⁽¹⁸⁾. Figure 6 shows the propagation of the

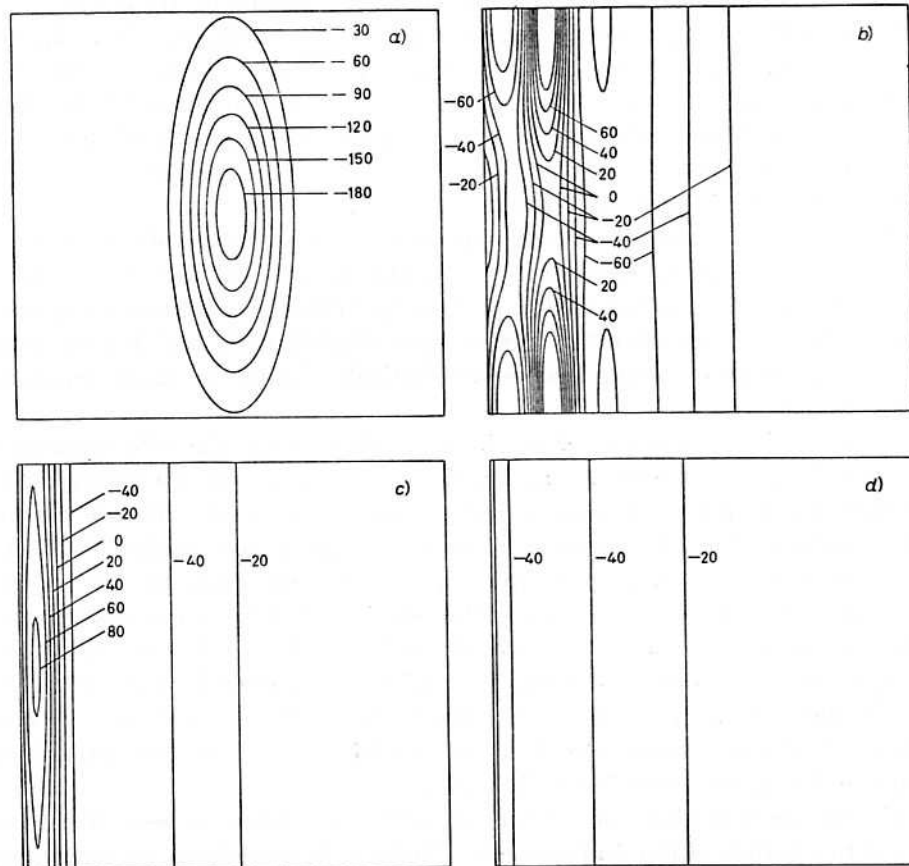


Fig. 6. - Contour lines of \tilde{E} in case E) (see test; $n_{t1\alpha} = 200$).

initial condition of the form (18) with the same parameters as in case A) except for A that now is $A = -0.2$. Also in this case the wave approaches a 2D state that coincides with the evolution of an «equivalent» 2D initial condition.

⁽¹⁷⁾ J. L. HAMMACK and H. SEGUR: *J. Fluid Mech.*, **84**, 359 (1978).

⁽¹⁸⁾ J. L. HAMMACK and H. SEGUR: *J. Fluid Mech.*, **84**, 337 (1978).

7. – Discussion and conclusions.

In this paper we have proposed a numerical scheme that solves the initial-boundary-value problem for a modified KP equation. Linear and nonlinear tests have been discussed. The evolution of a 3D initial condition has then been studied in a variety of cases and a 2D adjustment process has always been observed.

This agrees with the behaviour observed experimentally by HUANG *et al.* ⁽¹⁹⁾. An initial 3D travelling wave was generated by a ship model moving in a channel. For sufficiently high Froude numbers the wave proceeds ahead of the ship. Time series taken at two different points across the channel in the far field region show that the wave is strictly 2D, whereas the signals in the radiation field are uncorrelated (three-dimensionality). Further experimental evidence of this behaviour is given in ERTEKIN *et al.* ⁽²⁰⁾.

Apart from the above-mentioned experiments, there are also other numerical studies on this subject. ERTEKIN *et al.* ⁽²¹⁾ and KATSIS and AKYLAS ⁽²⁰⁾ model the effect of a ship moving down a channel by introducing a 3D moving pressure distribution and solve the forced Green-Naghdi (GN) and KP equation respectively, thus obtaining results qualitatively similar to those presented in this paper.

In discussing these properties in connection with the GN equations, ERTEKIN *et al.* ⁽²¹⁾ suggested a mathematical problem, *i.e.* « that of determining the class of equations that generate solitons ahead of a 3D disturbance moving along a canal, while still producing a complex wave pattern behind it ». Such a class of equations certainly comprehends the KP equation, as shown independently here and in ⁽¹⁹⁾. Moreover the solution of (12), (19) tends (in some norm) to the KdV evolution of some 2D initial condition. This mathematical property could turn out to be useful in applications where only the asymptotic state is relevant. In fact one should solve a 2D equation instead of a 3D one, provided that an appropriate KdV initial condition $\bar{E}(X, 0)$ can be determined from the KP initial condition $E(X, Y, 0)$.

Finally we note that the numerical method described in sect. 3 can be applied to a variety of physical problems. As far as fluid mechanics is concerned, it can find application in problems such as the propagation of tsunamis ⁽²²⁾,

⁽¹⁹⁾ D. B. HUANG, O. J. SIBUL, W. C. WEBSTER, J. V. WEHAUSEN, D. M. WU and T. Y. WU: *Conference on Behaviour of Ships in Restricted Waters, Varna*, Vol. 26 (1982), p. 1.

⁽²⁰⁾ R. C. ERTEKIN, W. C. WEBSTER and J. V. WEHAUSEN: *XV Symposium on Naval Hydrodynamics* (National Academy Press, Washington, D.C., 1985), p. 347.

⁽²¹⁾ R. C. ERTEKIN, W. C. WEBSTER and J. V. WEHAUSEN: *J. Fluid Mech.*, **169**, 275 (1986).

⁽²²⁾ S. PIERINI: to appear in *Ann. Ist. Univ. Nav. Napoli* (1986).

of long gravity waves in restricted and on shallow waters and of waves of interest in geophysical fluid dynamics (Rossby, topographically trapped, equatorial waves) that obey the KdV dynamics in many circumstances and for which, therefore, the KP equation could represent a useful refinement of the theory. Moreover, the present numerical scheme can be generalized to take into account further physical effects. The author is currently engaged in extending it to the case of waves travelling over 3D topographic variations.

* * *

This work originated from the intention to develop a 3D model of tsunami propagation. The author is very grateful to Prof. J. L. HAMMACK for having suggested the use of the KP equation, for many valuable conversations throughout the whole research and for useful comments on the manuscript. The author is also glad to acknowledge several helpful discussions with Prof. J. T. KIRBY. This research was supported by N.A.T.O. through a fellowship (n. 215.17/2) of the « Consiglio Nazionale delle Ricerche » of Italy and was carried out at the Dept. of Engineering Sciences of the University of Florida. The use of the computer facilities (VAX 750) provided in this Department is most gratefully acknowledged.

● RIASSUNTO

Si presenta uno schema alle differenze finite implicito e a tre livelli temporali per una versione regolarizzata dell'equazione Kadomtsev-Petviashvili, descrittiva della dinamica di una vasta classe di sistemi d'onda per i quali si hanno deboli effetti dispersivi, non lineari e tridimensionali. Una serie di test lineari e non lineari dà risultati numerici coincidenti con le corrispondenti soluzioni teoriche. Si analizza quindi l'evoluzione in un canale rettangolare di condizioni iniziali tridimensionali localizzate. In tutti i casi si osserva un processo di aggiustamento bidimensionale. Solitoni bidimensionali emergono rapidamente da onde iniziali positive. Ciò concorda con esperimenti di laboratorio. Inoltre il campo di radiazione si presenta sotto forma di onde tridimensionali simili alle soluzioni di Genus 2 dell'equazione KP.

Резюме не получено.